International Journal of Research
Available at https://edupediapublications.org/journals
e-ISSN: 2348-6848
p-ISSN: 2348-795X
Volume 04 Issue-17
December 2017

Three-Level Rectifiers in Wind Turbine Systems Open-Circuit Fault-Tolerant Control for Outer Switches

Jagruthi Petrum

[1] Assistant Professor with the Department of Electrical & Electronics Engineering at Dadi Institute of Engineering and Technology, JNT University, Kakinada, Andhra Pradesh, India,
E-mail id (petrumjagruthi@gmail.com)

Abstract- *The proposed tolerant control maintains normal operation with sinusoidal currents under the open-circuit fault of outer switches by adding a compensation value to the reference voltages. A three-level converter is used as the power converters of wind turbine systems because of their advantages such as low-current total harmonic distortion, high efficiency, and low collector–emitter voltage. Interior permanent magnet synchronous generators (IPMSGs) have been chosen as the generator in wind turbine systems owing to their advantages of size and efficiency. In wind turbine systems consisting of the three-level converter and the IPMSG, fault-tolerant controls for an open-circuit fault of switches should be implemented to improve reliability. This paper focuses on the open-circuit fault of outer switches (Sx1 and Sx4) in three level rectifiers (both neutral-point clamped and T-type) that are connected to the IPMSG. In addition, the effects of Sx1 and Sx4 open-circuit faults are analyzed, and based on this analysis, a tolerant control is proposed. The effectiveness and performance of the proposed tolerant control are verified by simulation*

IndexTerms—Neutral-point-clamped rectifier, open-circuit fault, open-switch fault, reliability, three-level topology, tolerant control, T-type rectifier.

NOMENCLATURE

pf Power factor.
Irec Rectifier input current.
*I x,*rec Rectifier input current of *x*-phase.
*V*rec Rectifier input voltage.
*V x,*rec Rectifier input voltage of *x*-phase. *V*EMF Back EMF of PMSG.
ϕZ Phase difference (°) between *V*EMF and *V*rec.
Φpf Phase difference (°) between *I*ref and *V*EMF.
V x ,ref Reference voltage of *x*-phase.
V mag Magnitude of the reference voltages.
fs Fundamental frequency (Hz) represented the angularfrequency of the PMSG.
*V*ref,max, Maximum and minimum values of *Va,*ref *V*ref,min *Vb,*ref , and *Vc,*ref .
V comp Compensation voltage of the proposed tolerant control.
R Equivalent resistance (Ω) of the PMSG.
L Equivalent inductance (H) of the PMSG.
I qe,Ide d-axis and *q*-axis currents in the d–q synchronous rotating frame.
*θ*EMF *V*EMF's angle.
Ma Modulation index, √3 × *V*mag/*V*dc.

I. INTRODUCTION

Improve the reliability of wind turbine systems. Switch faults are divided into a short-circuit fault and an open-circuit fault [12]. The short-circuit fault normally leads to a breakdown of the entire system; therefore, fault detection and tolerant control methods for the short-circuit fault require additional circuits. On the other hand, the open-circuit fault leads to current distortion, which can lead to a breakdown if it persists for a long time; therefore, the open-circuit fault should be detected, and the tolerant controls are necessary [9]. In wind turbine systems, a back-to-back converter is used to transfer power from the generator to the grid. A back-toback converter using the 3L-NPC topology The power capacity of a wind turbine system has been increasing consistently, leading to the development of generators with large power capacity [1]–[3]. There are many types of generators. Permanent magnet synchronous generators (PMSGs) have high efficiency and high reliability compared with induction generators. This is because external excitation is not required and there are no copper losses in the rotor circuits. Moreover, because of the smaller size of the PMSG, the weight of the wind turbine is reduced [4]. Among various PMSGs, interior PMSGs (IPMSGs) are especially advantageous from the standpoints of efficiency and power generation owing to the use of the reluctance torque [4]–[7]. Generators requiring high voltage need to use multilevel converter topologies to reduce the collector–emitter voltage per switch. Among multilevel topologies, three-level topologies such as the three-level neutral-point clamped (3L-NPC) and T-type topologies are applied in wind turbine systems with a wide power range. The three-level topology can easily be expanded from a two-level topology and is also easier to control compared with other multilevel topologies. Furthermore, the three-level topology guarantees high efficiency and low-current total harmonic distortion

International Journal of Research
Available at https://edupediapublications.org/journals
e-ISSN: 2348-6848
p-ISSN: 2348-795X
Volume 04 Issue-17
December 2017

(THD) in comparison with the two level topology [8]. The 3L-NPC topology is vulnerable to switch faults because many switches are used. Switch fault detection and tolerant control methods for switch faults should be implemented to improve the reliability of wind turbine systems. Switch faults are divided into a short-circuit fault and an open-circuit fault The short-circuit fault normally leads to a breakdown of the entire system; therefore, fault detection and tolerant control methods for the short-circuit fault require additional circuits. On the other hand, the open-circuit fault leads to current distortion, which can lead to a breakdown if it persists for a long time; therefore, the open-circuit fault should be detected, and the tolerant controls are necessary [9]. In wind turbine systems, a back-to-back converter is used to transfer power from the generator to the grid. A back-to-back converter using the 3L-NPC topology is shown in Fig. 1.

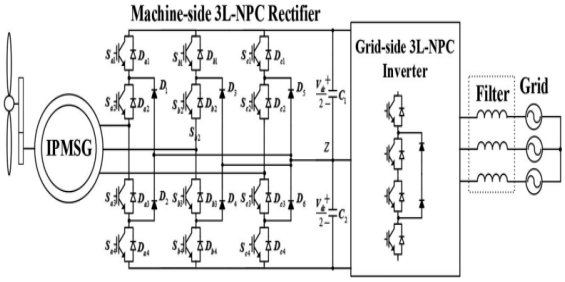

Fig. 1. Back-to-back converter using the 3L-NPC topology in wind turbine systems.

This consists of the machine-side 3L-NPC rectifier, the dc-link, and the grid-side 3L-NPC inverter. Depending on the operating conditions, tolerant controls can be applied for the rectifier or the inverter because the current paths of the rectifier and the inverter are different [9]. In addition, the different structure of the three-level topologies should be considered in the tolerant controls [9]. In the 3L-NPC inverter, the open-circuit fault of the inner switch causes the outer switch connected it to be infeasible; therefore, changing only the switching method does not become a solution for the open-circuit fault, and the additional devices such as fuses and switches should be added for achieving the tolerant operation under the open-circuit fault of the inner switch . However, the open-circuit fault of the outer switch can be handled by changed the switching method in limited rang, the tolerant control method limits the output voltage range by half. In the 3L-NPC rectifier, the current distortion caused by the open-circuit fault of the inner switch can be restored partially by clamping the switching state without any additional devices [2]. In addition, the reactive current is injected to eliminate current distortion caused by the open-circuit fault of the outer switch [2]. This method can also be applied for the T-type rectifier. The T-type rectifier is advantageous on the tolerant control because the switches in a leg are independent of each other. this control method injects the exact reactive current required to eliminate the current distortion. This means that the *pf* is changed. Rectifiers with IPMSGs can operate to generate maximum power at *pfs* other than unity. IPMSGs provide more power Many tolerant control methods for the open-circuit fault of the inner switch, which can be used in both the T-type inverter and rectifier, were proposed in [3], [4], and [2]–[5]. These methods change the switching method to disable the switch with the open-circuit fault and do not need the additional devices. This paper focuses on the open-circuit fault of the machine side 3L-NPC rectifier. In general, the input currents of the 3LNPC rectifier do not flow through the outer switches (*Sx*1 and *Sx*4) at unity power factor (*pf*); therefore, the existing tolerant controls for the 3L-NPC rectifier take into account only the inner switches (*Sx*2 and *Sx*3) [3]. However, according to the specification of the PMSG, an open-circuit fault of the outer switch can cause current distortion as much as when an open circuit fault of the inner switch occurs [2]. The tolerant control for *Sx*1 and *Sx*4 open-circuit faults is also proposed

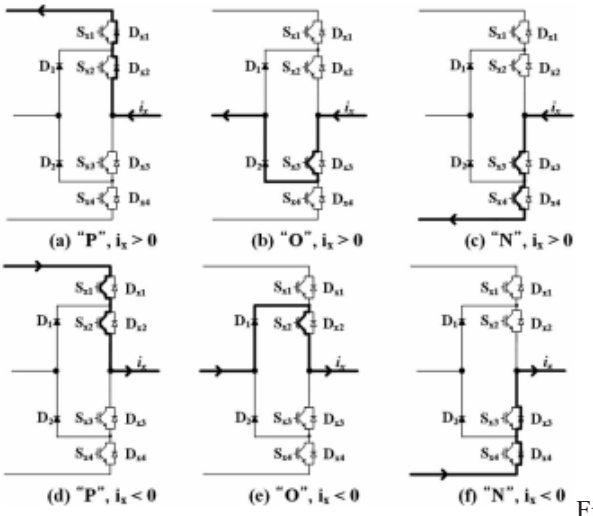

Fig. 2. Current paths depending on the current direction and the switching state.

when rectifiers operate at a unique *pf* [4]–[7]. In such a case, an open-circuit fault of the outer switches (*Sx*1 and *Sx*4) causes current distortion and torque fluctuation, which can lead to vibration of the wind turbine. In this paper, the reason for the current distortion caused by the outer switches (*Sx*1 and *Sx*4) is analyzed, and then, on the basis of this analysis, a tolerant control for *Sx*1 and *Sx*4 open-circuit faults is

International Journal of Research
Available at https://edupediapublications.org/journals
e-ISSN: 2348-6848
p-ISSN: 2348-795X
Volume 04 Issue-17
December 2017

proposed. In the proposed tolerant control, the switch with an open-circuit fault is not used to generate the input voltages of the three-level rectifier by adding a compensation value to the reference voltages. The compensation value is simply calculated and the *pf* does not change in the proposed tolerant control. The performance of the proposed tolerance control is proved by simulation.

II. OPEN-CIRCUIT FAULT ANALYSIS OF OUTER SWITCHES

There are three switching states (P, N, and O) in the 3L-NPC rectifier [9]. Six current paths can be generated depending on the current direction and the switching state, and these are shown in Fig. 2 [3]. Fig. 3 shows the input current generation process of a rectifier with unity *pf*. The rectifier current is *I*rec, the rectifier voltage is *V*rec, and the back electromotive force (EMF) is *V*EMF. The

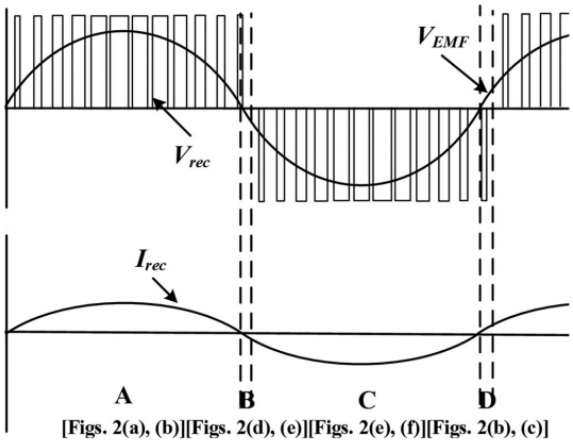

Fig. 3. Rectifier operation at unity *pf*

TABLE I
CURRENT PATH COMPOSITION DEPENDING ON THE PART OF FIG. 3

Part	V_{rec}	I_{rec}	Current path
A	Positive	Positive	(a) P switching state, (b) O switching state (valid)
B	Positive	Negative	(d) P switching state (valid), (e) O switching state
C	Negative	Negative	(e) O switching state (valid), (f) N switching state
D	Negative	Positive	(b) O switching state, (c) N switching state (valid)

The current continuously flows through two diodes if the switching state is changed to P or N switching state in which no current flows through the switches. In parts B and D, the P and N switching stages are the valid switching state where the current flows through the switches. Phase difference between *V*EMF and *V*rec, which causes the current flow, is controlled to match the phase of *I*rec up with the phase of the corresponding *V*EMF. One period of *I*rec can be divided into four parts depending on the polarity of *I*rec and *V*rec. The generated current paths are different depending on the part, and these are summarized in Table I. In parts A and C, the O switching state causes the input current flow; therefore, this is called the valid switching state. When the rectifier operates with unity *pf*, parts A and C are large, and parts B and D are small. If parts B and C are very small as much as be ignored, the *Sx*1 and *Sx*4 open-circuit faults can be ignored [22], [23]. However, parts B and D can be extended in Case I when *V*EMF is small and a large *I*rec is required [22]. This is because the phase difference between *V*EMF and *V*rec becomes large. In

this paper, the other case (Case II), which is the reactive current injection for IPMSG, is also considered. Fig. 4 shows that the input current generation process of the rectifier for Cases I and II. There are two phase differences: the phase difference (ϕZ) between *V*EMF and *V*rec explained in [22], and the phase difference (ϕpf) between *I*ref and *V*EMF caused by the *pf*. In Fig. 4, part B (or part D) consists of ϕZ and ϕpf , and their lengths increase. This means that the current can be more distorted by the open-circuit fault of the outer switches compared to when

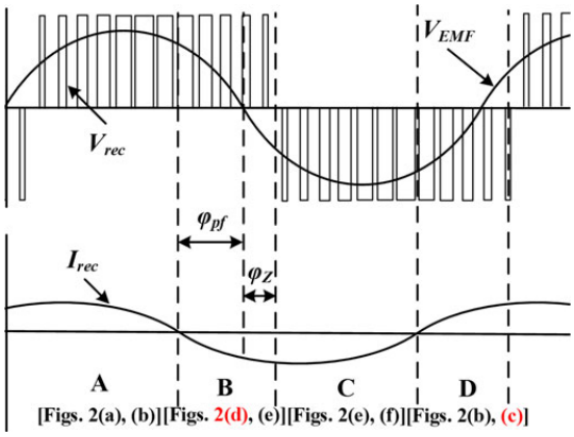

Fig. 4. Rectifier operation at any *pf*

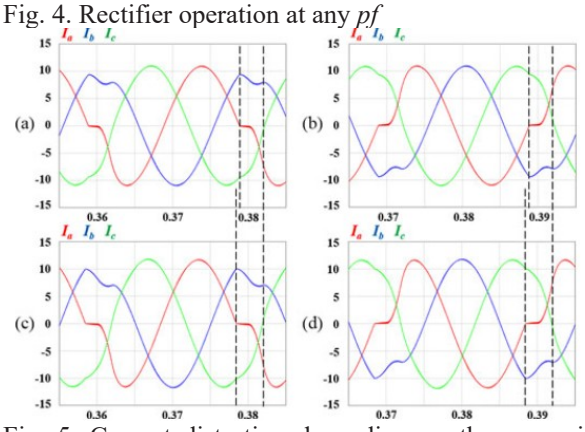

Fig. 5. Current distortion depending on the open-circuit fault and the *pf*: (a) 0.95 *pf*, *Sx*1 open-circuit fault, (b) 0.95 *pf*, *Sx*4 open circuit fault, (c) 0.9 *pf*, *Sx*1 open-circuit fault, and (d) 0.9 *pf*, *Sx*4 open-circuit fault. ϕZ alone is considered. Case I can be ignored because ϕZ is determined depending on the operating condition of the rectifier and the PMSG. However, because ϕpf is

International Journal of Research
Available at https://edupediapublications.org/journals
e-ISSN: 2348-6848
p-ISSN: 2348-795X
Volume 04 Issue-17
December 2017

determined by the *pf*, Case II should be considered when the IPMSG is employed. The current distortion caused by the open-circuit fault of the outer switches is shown in Fig. 5 for various *pfs*. Owing to the infeasible open-circuit fault switch, the current becomes zero during the range consisting of ϕZ and ϕpf . The *Sx*1 open-circuit fault makes the current path of Fig. 2(d) infeasible. The current path of Fig. 2(d) belongs to part B; therefore, the *Sx*1 open circuit fault causes distortion in the negative current as shown in Fig. 5(a) and (c). On the contrary, the *Sx*4 open-circuit fault leads to distortion in the positive current as shown in Fig. 5(b) and (d) because the current path of Fig. 2(c) related to the *Sx*4 open-circuit fault belongs to part D. The low *pf* has a large ϕpf . Therefore, the rectifier operation at a low *pf* leads to a large zero-current range when the open circuit fault of the outer switch occurs. As a result, the zero current range increases, as the *pf* decreases. The analysis related to the open-circuit fault of the outer switches can be applied to the T-type topology. The effects of open-circuit faults of the outer switches on the current are the same in both the NPC rectifier and the T type rectifier [3], [2]. Therefore, the current distortion caused by open-circuit faults of the outer switches in the NPC rectifier is the same as that in the T-type rectifier.

III. TOLERANT CONTROL FOR OPEN-CIRCUIT FAULT OF OUTER SWITCHES

This method changes the phase of *I*rec so that it corresponds with the phase of *V*rec. This means that parts B and D are eliminated. An existing tolerant control method for the open-circuit fault of the outer switches is reactive current injection [2]. However, this tolerant control method has the disadvantage of low-power generation efficiency of the generator because the PMSG has efficient operating condition which depends on the *pf* of the rectifier. In general, the unity *pf* is required for the best operating condition of a surface PMSG. The best operating condition of an IPMSG does not correspond to the unity *pf*, and this is determined by the specifications of the IPMSG. The proposed tolerant control does not change the *pf* of the rectifier. The rectifier voltage (*V*rec) without the current path related to the open-circuit fault switch is generated by changing the reference voltages. To explain the proposed tolerant control, the *Sx*1 open-circuit fault is used as an example.

*A. Compensation Voltage (V*comp*) Calculation*

In the proposed tolerant control, a reference voltage of a phase containing the *Sx*1 Fig. 6. Change of reference voltages in the proposed tolerant control for the *Sx*1 open-circuit fault (0.95 *pf*). open-circuit fault is changed to zero as shown in Fig. 6. is the fundamental frequency. The offset voltage (*V*offset) is added to each reference voltage to expand the range of the modulation index ($Ma = \sqrt{3} \times V$ mag/*V*dc). *V*offset and the changed reference voltages (*Vx*,ref,offset, *x* = *a, b, c*) are expressed as

*V*offset = -(*V*ref,max + *V*ref,min)/2, (2)

V a,ref,offset = *Va*,ref + *V*offset

Vb,ref,offset = *Vb*,ref + *V*offset *V c*,ref,offset = *Vb*,ref + *V*offset (3)

where *V*ref,max and *V*ref,min are the maximum and minimum values of *V a*,ref , *Vb*,ref , and *Vc*,ref . The reference voltages of (3) are compared with the carrier signals to generate *V*rec. When the *Sx*1 open-circuit fault occurs, the current path of Fig. 2(d) should be eliminated to prevent current distortion; therefore, the reference voltage should be changed to generate *V*rec without the current path of Fig. 2(d). As a result, the current path of Fig. 2(d) disappears because the O switching state is only used in part B. To make the reference voltage zero, |*V*comp| is assigned the magnitude of the reference voltage (*Vx*,ref,offset) containing the open-circuit fault, and *V* comp can be expressed as

V comp = -*V*x,ref,offset(*x* = a phase containing open -circuited fault switch). (4)

The proposed tolerant control is implemented by adding *V* comp to the reference voltages (*Vx*,ref,offset, *x* = *a, b, c*). The new reference voltages (*Vx*,ref,tolerance, *x* = *a, b, c*) of the proposed tolerant control are expressed as

V c,ref,tolerance = *Vb*,ref,offset + *V*comp. (5)

*B. Compensation Range for Adding V*comp

By adding *V*comp to each reference voltage, the use of the current path related to the open-circuit fault switch will be precluded. To achieve this perfectly, *V*comp is added for the suitable range and position. The compensation range, which is part B or part D of Fig. 4, consists of ϕZ and ϕpf . ϕZ can be calculated with the equivalent circuit of the PMSG and the three-level rectifier [22]. ϕZ , which is the phase difference between *V*EMF and *V*rec, is expressed as

ϕZ = tan-1 - | *V*EMF *I*rec| × - |*I*2ref $\pi f|sRL$ (6)

where *R* and *L* are the equivalent resistance and inductance of the PMSG, and *fs* is the fundamental frequency representing the angular frequency of the PMSG. ϕpf , which is the phase difference between *V*EMF and *I*rec, is related to the *pf*. ϕpf can be calculated by the *pf* and this is

International Journal of Research
Available at https://edupediapublications.org/journals
e-ISSN: 2348-6848
p-ISSN: 2348-795X
Volume 04 Issue-17
December 2017

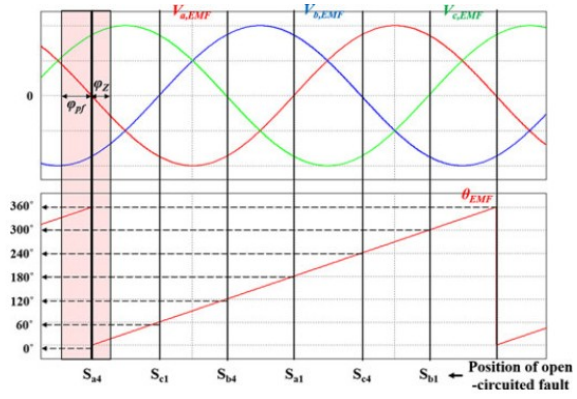

Fig. 7. Compensation position on the basis of *V*EM F 's angle (*θ*EM F).

expressed as ϕpf = cos-1(pf). (7) If the d–q control theorem is used, ϕpf can be calculated as $\phi pf = \cos^{-1}\left(\frac{Iqe\ 2Iqe + Ide\ 2}{}\right)$, (8) where *Ide* indicates the *d*-axis current related to the flux and *Iqe* indicates the *q*-axis current related to the torque, and these are values in the d–q synchronous rotating frame. ϕZ andϕpf , which are calculated from (6) and (8), are located near the zero-crossing point of *V*EMF as shown in Fig. 6. Therefore, the compensation position for adding *V*comp is defined on the basis of *V*EMF's angle (*θ*EMF). Fig. 7 shows three-phase *V*EMF*s* and *θ*EMF. *θ*EMF is acquired from the encoder or position sensor. Six zero-crossing points are expressed for every 60°, which are matched to each open-circuit fault as shown in Fig. 7. Consequently, *θ*EMF representing each zero-crossing point is a criterion for adding *V*comp. For example, when the *Sa*1 open circuit fault occurs, *V*comp should be added for the compensation range from (0◦ - ϕpf) to (0◦ + ϕZ) which is based on 0°. By considering all open-circuit faults, Table II shows the compensation ranges for eliminating the current distortion depending on the position of the open-circuit fault.

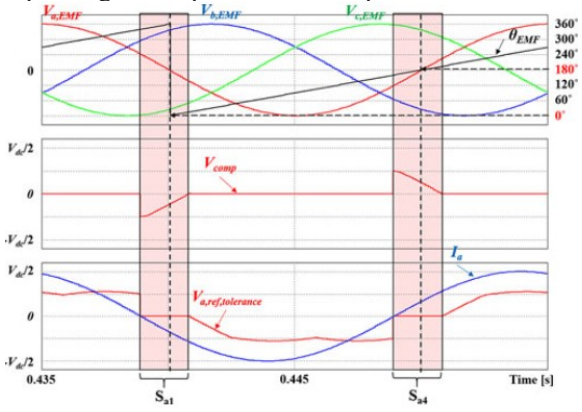

Fig. 8. Proposed tolerant control considering neutral-point voltage balance under the *Sa*1 open-circuit fault.

C. Considering Neutral-Point Voltage Balance

The compensation voltage which is one of the offset voltages can cause neutral-point voltage unbalance because *V*comp calculated from (4) is a one-sided voltage [1], [4]. Therefore, two dc-link capacitors have different values depending on the polarity of *V*comp generated for the open-circuit fault. The neutral-point voltage unbalance increases the voltage stress on the switch and the current THD [24]. The proposed tolerant control for the open-circuit fault of the outer switches has to incorporate a solution for the neutral point voltage unbalance problem. Therefore, as mentioned earlier, *V*comp is added for the corresponding compensation position depending on the position of the open-circuit fault, and then, *V*comp is also added in the diametrically opposite compensation position to balance the neutral-point voltage. Two *V*comps added in two positions have opposite polarity, and this results in the balanced neutral-point voltage. The final principles of the proposed tolerant control with the neutral-point voltage balance are summarized in Table III.

Fig. 8 shows the concept of proposed tolerant control considering the neutral-point voltage balance when the *Sa*1 open-circuit fault occurs. In Fig. 8, *V*comp is added for the compensation range [(0◦ - ϕpf) ∼ (0◦ + ϕZ)] which corresponds to the position for the *Sa*1 open-circuit fault; in addition, *V*comp is also added for the diametrically opposite compensation range [(180◦ - ϕpf) ∼ (180◦ + ϕZ)], which is the range for the *Sa*4 open-circuit fault.

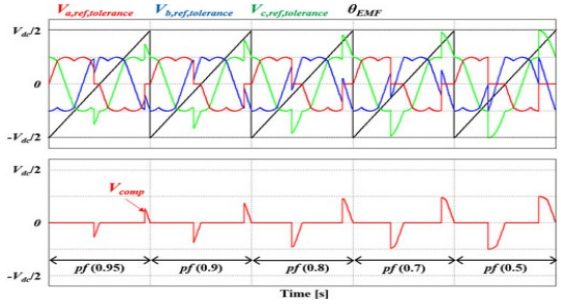

Fig. 9. *Vx,*ref,tolerance (x = a,b,c) and *V*com p depending on the *pf* when *Ma* is 0.5.

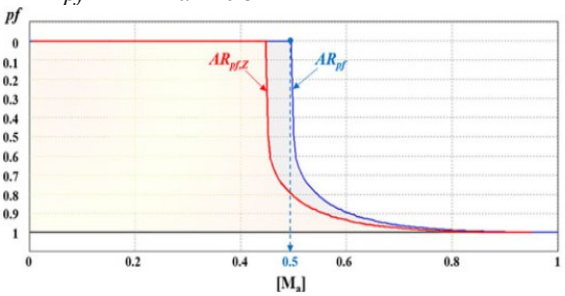

Fig. 10. Applicable *pf* range of the proposed tolerant control depending on *Ma* .

D. Limitation of Proposed Tolerant Control

International Journal of Research
Available at https://edupediapublications.org/journals
e-ISSN: 2348-6848
p-ISSN: 2348-795X
Volume 04 Issue-17
December 2017

V x,ref,tolerance cannot exceed a limitation voltage (*V*limit), which is restricted by the dc-link voltage (*V*dc). Therefore,*V*comp is limited as follows: *V*comp < *V*limit - *V*ref,max (9) where *V*limit is *V*dc/2. On the basis of (9), the applicable operation range of the proposed tolerant control is determined depending on *Ma* and the *pf*. Fig. 9 shows *Vx*,ref,tolerance and *V*comp of the proposed tolerant control depending on the *pf* when *M*a is 0.5. In Fig. 9, *V*comp leads to *V a*,ref,tolerance with zero value in the corresponding compensation range. Moreover, the peak value of *Vc*,ref,tolerance increases owing to *V*comp. As the *pf* decreases, this peak value increases; however, it does not exceed *V*limit. Consequently, when *Ma* is smaller than 0.5, *V*comp can be added regardless of the *pf* because *Vc*,ref,tolerance cannot exceed *V*limit. When *Ma* is larger than 0.5, the applicable *pf* range is determined by *Ma*.

This is because a low *Ma* provides a large margin for *V*comp; however, a large *V*comp cannot be acceptable for high *Ma*. Fig. 10 shows the applicable *pf* range for various values of*Ma*. The shaded part of Fig. 10 represents the applicable operation range. The proposed tolerant control is feasible over the entire factor range when *Ma* is smaller than 0.5. By increasing *Ma* from 0.5, the applicable operation range decreases. In Fig. 10

TABLE IV
IPMSG PARAMETERS IN SIMULATION

Rated power	2.5 MW
Number of pole	8
Rated voltage (line-to-line)	760 V_{rms}
Rated current	1902 A_{rms}
Rated speed	1650 rpm
Resistance	0.4567 mΩ
q-inductance	0.0982 mH
d-inductance	0.0725 mH

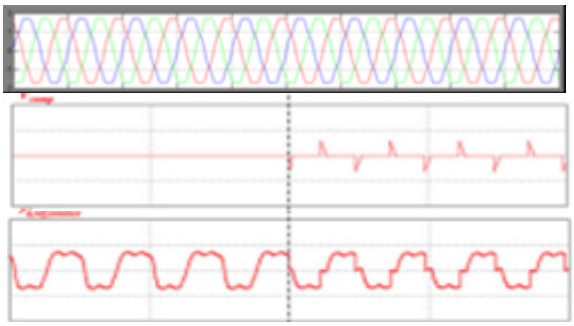

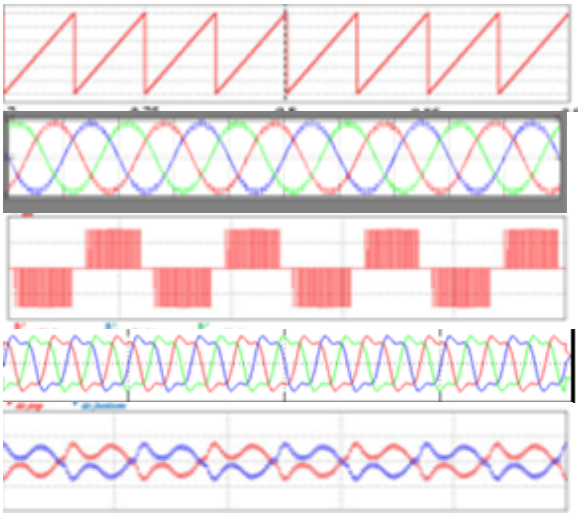

Fig. 11. Simulation results with the proposed tolerant control under the *Sa*1 open-circuit fault (600 rpm, *Ma* = 0.35, 0.95 *pf*)

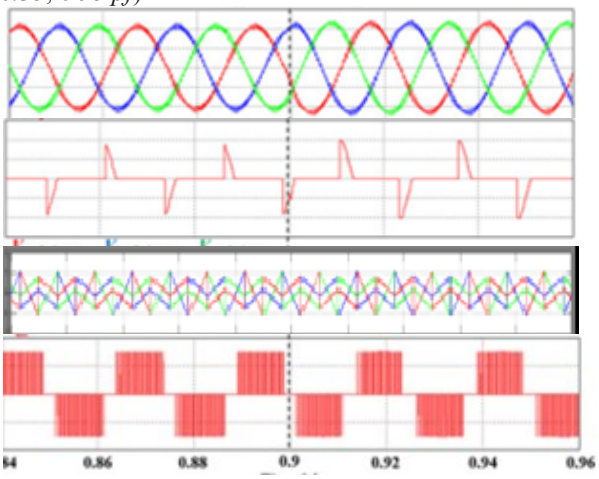

Fig. 12. Simulation results with the proposed tolerant control under the *Sa*1 open-circuit fault (600 rpm, *Ma* = 0.35, *pf*-transition from 0.95 to 0.9).

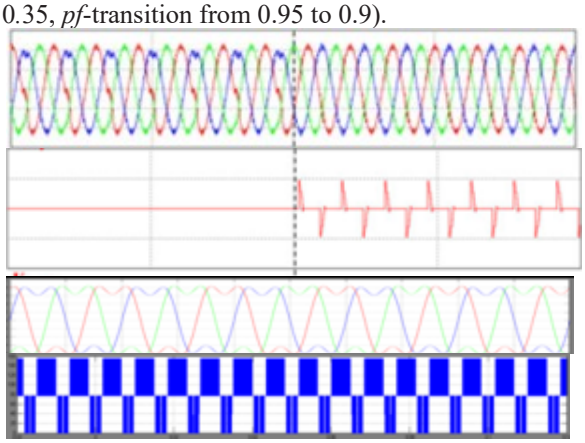

Fig. 13. Simulation results with the proposed tolerant control under the *Sa*1 open-circuit fault (1000 rpm, *Ma* = 0.59, 0.95 *pf*)

IV. SIMULATION RESULTS

The simulation is performed using the PSIM tool. The 3L-NPC rectifier of the back-to back converter with 2.5-MW IPMSG is only considered in the simulation. *pfs* and generator speeds. of the PMSG is 600 rpm, *Ma* is 0.35, and the *pf* of the rectifier is 0.95. Owing to the *Sa*1 open-circuit fault, the negative current is distorted as shown in Fig. 11(a). After the reference voltages are changed by *V*comp for the corresponding ranges $[(0^\circ - \phi pf) \sim (0^\circ + \phi Z), (180^\circ - \phi pf) \sim (180^\circ + \phi Z)]$ which are defined in Table III. As a result, the a-phase pole voltage (*Van*) is clamped to 0 at their ranges as shown in Fig. 11(b) and the current distortion is eliminated completely. In addition, the two dc-link capacitor voltages are balanced. The simulation parameters are as follows: the switching frequency is 2 kHz, the control period is 250 μs, the dc-link capacitor is 35 mF, and the dc-link voltage is 1200 V. The IPMSG parameters used in the simulation are shown in Table IV. The proposed tolerant control for the open-circuit fault of the outer switches (*Sx*1,*Sx*4) is implemented for different The proposed tolerant control is effective for the *pf* transition operation of the rectifier. Fig. 12 shows the results when the proposed tolerant control is applied and the *pf* is changed from 0.95 to 0.9. The compensation the *pf* decreases and the currents are maintained without distortion continuously. Moreover, we know that the peak value of *V c,*ref,tolerance becomes large because the *pf* decreases which was discussed in Section III. The proposed tolerant control is applied. The current THD is increased by the *Sa*1 open-circuit fault; however, owing to the proposed tolerant control, the current THD is restored as good as normal state without any open-circuit fault.

VI.CONCLUSION

This paper proposes a tolerant control for the open-circuit fault of the outer switches in three-level rectifiers (both 3L-NPC and T-type topologies) used in wind turbine systems This control is implemented by adding a compensation voltage (*V*comp) to the reference voltages for the corresponding compensation ranges depending on the position of the open-circuit fault. Furthermore, this control can be used in both the 3L-NPC. The reason why the tolerant control for the open-circuit fault of the outer switches in three-level rectifiers is necessary is presented, together with the supporting circuit analysis. and T-type rectifiers and guarantees normal operation without a change of the *pf* in the applicable operation range shown in Fig. 10 depending on the modulation index (*Ma*) and the *pf*. Although the operating range of the proposed tolerant control is subject to a limitation, not always operate with the rated wind speed and that the operating *pf* of the rectifier with an IPMSG is not too low, the proposed tolerant control is clearly effective. The performance and of the proposed tolerance control are simulations.

REFERENCES

[1] A. Isidori, F. M. Rossi, F. Blaabjerg, and K. Ma, "Thermal loading and reliability of 10-MW multilevel wind power converter at different wind roughness classes," *IEEE Trans. Ind. Appl.*, vol. 50, no. 1, pp. 484–494, Jan./Feb. 2014.

[2] H. G. Jeong, K. B. Lee, S. Chio, and W. Choi, "Performance improvement of LCL-filter-based grid-connected inverters using PQR power transformation," *IEEE Trans. Power Electron.*, vol. 25, no. 5, pp. 1320–1330, May 2010.

[3] S. Li, T. A. Haskew, R. P. Swatloski, and W. Gathings, "Optimal and direct-current vector control of direct-driven PMSG wind turbines," *IEEE Trans. Power Electron.*, vol. 27, no. 5, pp. 2325–2337, May 2012.

[4] W. Qiao, L. Qu, and R. G. Harley, "Control of IPM synchronous generator for maximum wind power generation considering magnetic saturation," *IEEE Trans. Ind. Appl.*, vol. 45, no. 3, pp. 1095–1105, May/Jun. 2009.

[5] S. Morimoto, H. Nakayama, M. Sanada, and Y. Takeda, "Sensorless output maximization control for variable-speed wind generation system using IPMSG," *IEEE Trans. Ind. Appl.*, vol. 41, no. 1, pp. 60–67, Jan./Feb. 2005.

[6] Y. Zhao, W. Qiao, and L. Wu, "An adaptive quasi-sliding-mode rotor position observer-based sensorless control for interior permanent magnet synchronous machines," *IEEE Trans. Power Electron.*, vol. 28, no. 12, pp. 5618–5629, Dec. 2013.

[7] P. B. Reddy, A. M. EL-Refaie, and K. K. Huh, "Effect of number of layers on performance of fractional-slot concentrated-windings interior permanent magnet machines," *IEEE Trans. Power Electron.*, vol. 30, no. 4, pp. 2205–2218, Apr. 2015.

[8] J. S. Lee and K. B. Lee, "New modulation techniques for a leakage current reduction and a neutral-point voltage balance in transformerless photovoltaic systems using a three-level inverter," *IEEE Trans. Power Electron.*, vol. 29, no. 4, pp. 1720–1732, Apr. 2014.

[9] U. M. Choi, H. G. Jeong, K. B. Lee, and F. Blaabjerg, "Method for detecting an open-switch fault in a grid-connected NPC inverter system," *IEEE Trans. Power Electron.*, vol. 27, no. 6, pp. 2726–2739, Jun. 2012.

[10] U. M. Choi, J. S. Lee, and K. B. Lee, "New modulation strategy to balance the neutral-point voltage for three-level neutral-clamped inverter systems," *IEEE Trans. Energy Convers.*, vol. 29, no.